Chemical Research in Toxicology

Article

pubs.acs.org/crt

Simultaneous Detection of Deoxyadenosine and Deoxyguanosine Adducts in the Tongue and Other Oral Tissues of Mice Treated with Dibenzo[*a*,*l*]pyrene

Shang-Min Zhang,[†,§] Kun-Ming Chen,[†,§] Yuan-Wan Sun,[†] Cesar Aliaga,[†] Jyh-Ming Lin,[†] Arun K. Sharma,[‡] Shantu Amin,[‡] and Karam El-Bayoumy*[,†]

[†]Dept. of Biochemistry and Molecular Biology, Penn State College of Medicine, Hershey, Pennsylvania 17033, United States

[‡]Dept. of Pharmacology, Penn State College of Medicine, Hershey, Pennsylvania 17033, United States

Supporting Information

ABSTRACT: We were the first to demonstrate that direct application of the environmental pollutant and tobacco smoke constituent dibenzo[*a*,*l*]pyrene (DB[*a*,*l*]P) into the oral cavity of mice induced squamous cell carcinoma (SCC) in oral tissues but not in the tongue; however, the mechanisms that can account for the varied carcinogenicity remain to be determined. Furthermore, we also showed that not only dA adducts, but also dG adducts can account for the mutagenic activity of DB[*a*,*l*]P in the oral tissues *in vivo*. In this study, we initially focused on DB[*a*,*l*]P-induced genotoxic effects in both oral and tongue tissues. Therefore, to fully assess the contribution of these DNA adducts in the initiation stage of carcinogenesis induced by DB[*a*,*l*]P, an LC-MS/MS method to simultaneously detect and quantify DB[*a*,*l*]PDE-dG and -dA adducts was developed. Mice were orally administered with DB[*a*,*l*]P (24 nmole, 3 times per week for 5 weeks) or its fjord region diol epoxide, (±)-*anti*-11,12-dihydroxy-13,14-epoxy-11,12,13,14-tetrahydrodibenzo[*a*,*l*]-pyrene (DB[*a*,*l*]PDE, 12 nmole, single application); animals were sacrificed at 2, 7, 14, and 28 days after the last dose of carcinogen administration. Oral and tongue tissues were obtained and DNA were isolated followed by enzymatic hydrolysis. Following the development of an isotope dilution LC-MS/MS method, we successfully detected (−)-*anti-cis*- and (−)-*anti-trans*-DB[*a*,*l*]PDE-N^2-dG, as well as (−)-*anti-cis*- and (−)-*anti-trans*-DB[*a*,*l*]PDE-N^6-dA in oral and tongue tissues of mice treated with DB[*a*,*l*]P. Levels of (−)-*anti-trans*-DB[*a*,*l*]PDE-N^6-dA were ≥2 folds higher than (−)-*anti-cis*-DB[*a*,*l*]PDE-N^6-dA adduct and those of dG adducts in the oral tissues and tongue at all time points selected after the cessation of DB[*a*,*l*]P treatment. Levels of dG adducts were comparable in both tissues. Collectively, our results support that DB[*a*,*l*]P is predominantly metabolized to (−)-*anti*-DB[*a*,*l*]PDE, and the levels and persistence of (−)-*anti-trans*-DB[*a*,*l*]PDE-N^6-dA may, in part, explain the carcinogenicity of DB[*a*,*l*]P in the oral tissues but not in the tongue.

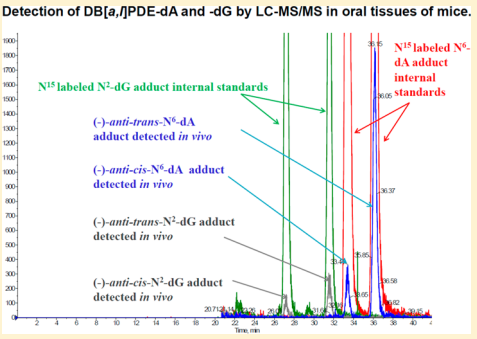

INTRODUCTION

It is estimated that about 174 100 cancer deaths will be caused by tobacco use in 2013;[1] all forms of smoked and smokeless tobacco products are known risk factors of oral cancer.[2] The U. S. Surgeon General's report has outlined that tobacco carcinogens such as polycyclic aromatic hydrocarbones (PAHs) and tobacco specific nitrosamines (TSNA) are the most likely causes of oral cancer.[3] Dibenzo[*a*,*l*]pyrene (DB-[*a*,*l*]P), a representative example of PAHs, is an environmental pollutant and a tobacco smoke constituent;[4−7] although not quantified, it was identified in cigarette smoke.[8] Animal studies have shown that DB[*a*,*l*]P is the most potent carcinogenic PAH tested so far, inducing tumors in mouse skin, lungs, and ovaries,[9,10] as well as rat mammary glands.[6] In addition, we recently demonstrated that DB[*a*,*l*]P is capable of inducing squamous cell carcinoma (SCC) in the oral tissues but not in the tongue of mice.[11]

It is generally accepted that PAHs exert their mutagenic effects and initiate the carcinogenic process through the generation of active metabolites that lead to the formation of potentially mutagenic covalent DNA adducts, which can cause miscoding and mutations.[12] Among the variety of PAH metabolites, diol-epoxides are often the major ultimate carcinogens.[6] Recently, we have also shown that direct application of the fjord region diol epoxide, (±)-*anti*-11,12-dihydroxy-13,14-epoxy-11,12,13,14-tetrahydrodibenzo[*a*,*l*]-pyrene (DB[*a*,*l*]PDE), a metabolite of DB[*a*,*l*]P, induced SCC in both tongue and other oral tissues in the mouse.[13] At the higher dose (6 nmole, 3× per week for 38 weeks), DB[*a*,*l*]PDE induced 74% SCC in the tongue, but it induced 100% SCC in other oral tissues; the corresponding values at the lower dose (3 nmole) were 45% and 89%.[13] We concluded that the formation of diol epoxides plays a major role in the initiation stage of DB[a,l]P-induced carcinogenicity.[13] However, the mechanisms that can account for the varied carcinogenicity in tongue and

Received: March 21, 2014
Published: June 9, 2014

   dx.doi.org/10.1021/tx5001078 | *Chem. Res. Toxicol.* 2014, 27, 1199−1206

Chart 1. Structures of DNA Adducts Derived from (±)-*anti*-DB[*a*,*l*]PDE *in Vivo*

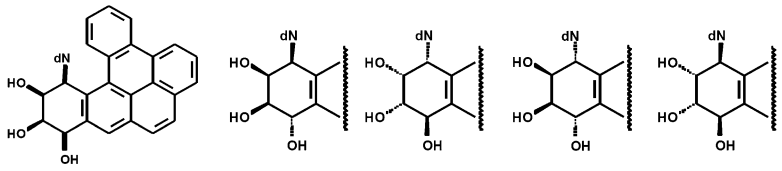

other oral tissues of mice treated with DB[a,l]P remain unknown.

Subsequently, we reported the mutagenicities in c*II* gene of the oral cavity of B6C3F1 (Big Blue) mice treated with DB[*a*,*l*]P or (±)-*anti*-DB[*a*,*l*]PDE.[11,13] DB[*a*,*l*]P and (±)-*anti*-DB[*a*,*l*]PDE both induced more mutations at GC base pairs than AT base pairs, but they induced significantly higher fraction of mutations at AT base pairs compared to benzo[*a*]pyrene (B[*a*]P). These results indicate the importance of both DB[*a*,*l*]PDE-dG and dA adducts in inducing mutations, suggesting that both types of adducts can be persistent long enough in the genome to induce mutations. Therefore, to fully assess the contribution of both dG and dA adducts in the initiation stage of carcinogenesis, it is important to develop a sensitive method to identify and quantify both *anti*-DB[*a*,*l*]-PDE-dG and dA adducts simultaneously in the tongue and other oral tissues of mice treated with DB[*a*,*l*]P.

The quantitation of DNA adducts derived from tobacco products (*N*′-nitrosonornicotine) in the oral cavity of rats during a carcinogenicity study by LC-MS/MS has provided better mechanistic insights on the role of these adducts in oral carcinogenesis.[14] We also reported the detection and quantification of DB[*a*,*l*]PDE-dA adducts in the oral tissues of mice treated with DB[*a*,*l*]P and (±)-*anti*-DB[*a*,*l*]PDE.[15] In the present report, we developed a LC-MS/MS method to simultaneously detect and quantify DB[*a*,*l*]PDE-dA and dG adducts in the tongue and other oral tissues of mice treated with DB[*a*,*l*]P. The internal standard [$^{15}N_5$]-(±)-*anti*-DB[*a*,*l*]-PDE-N^2-dG adducts were synthesized, and the stereochemistry of each isomer was characterized by mass spectrometry (MS), nuclear magnetic resonance (NMR), and circular dichroism (CD) analysis, according to published procedures.[16] In addition, to understand the biological fate of these adducts, we compared the formation and disappearance of both dG and dA adducts as a function of time after cesation of carcinogen treatment in the tongue and other oral tissues of mice treated with DB[*a*,*l*]P.

MATERIALS AND METHODS

Caution: DB[a,l]P and DB[a,l]PDE are mutagenic and carcinogenic. They should be handled with extreme care, following NCI safety http://pubs.acs.org/doi/abs/10.1021/ed052pA419.

Chemicals. DB[*a*,*l*]P and (±)-*anti*-DB[*a*,*l*]PDE were prepared according to a published method by our group.[17] [$^{15}N_5$]-dG were obtained from Spectra Stable Isotopes (Columbia, MD). Solvents, other chemicals and enzymes used in the present study were obtained from Sigma-Aldrich (St. Louis, MO). DB[*a*,*l*]PDE-N^6-dA adduct standards including [$^{15}N_5$]-DB[*a*,*l*]PDE-N^6-dA adducts were prepared as previously reported.[15]

Synthesis and Structural Characterization of dG Adduct Standards. (±)-*anti*-DB[*a*,*l*]PDE-N^2-dG adducts (see Chart 1) were prepared according to a method published previously.[16] They were synthesized by adding racemic (±)-*anti*-DB[*a*,*l*]PDE [5 mg, dissolved in 1 mL of dry dimethylformamide (DMF) under N_2] to excess dG (35 mg) at 100 °C for 30 min. DMF was then removed under vacuum; the residue was dissolved in DMSO/CH_3OH (1:1). Purification methods, HPLC analysis and spectral analyses (UV, CD, NMR, and MS) used for dG adducts were identical to those used for dA adducts described before.[15] The ^{1}H NMR spectra of the dG adducts were recorded in DMSO-d6 at 600 MHz on a Bruker Avance NMR spectrometer. The concentration of each purified stereoisomer was determined by UV spectroscopy (Beckman Coulter DU 640 spectrophotometer), (ε = 42000 M^{-1} cm^{-1}).[18] The MS/MS analysis was conducted by an API 3200 LC/MS/MS triple quadrupole mass spectrometer (Applied Biosystem). The CD spectra were recorded in methanol on a Jasco J-815 CD spectrometer. The ^{15}N-labeled internal standard [$^{15}N_5$]-(±)-*anti*-DB[*a*,*l*]PDE-N^2-dG adducts were prepared and characterized essentially following the same approach described above for unlabeled dG adducts, except using [$^{15}N_5$]-deoxyguanine (Cambridge Isotope Laboratories, Andover, MA), .

Detection and Quantification of *anti*-DB[*a*,*l*]PDE-N^2-dG Adducts in Vivo. Mice were treated with DB[*a*,*l*]P and (±)-*anti*-DB[*a*,*l*]PDE as reported previously.[13] In brief, female B6C3F1 mice (Jackson Laboratories, Bar Harbor, ME), 6 weeks of age, were used in bioassays. A group of three mice was treated topically with a single dose of 12 nmol of DB[*a*,*l*]PDE into the oral cavity and sacrificed at 48 h after the treatment. Another group of three mice was treated with 240 nmol DB[*a*,*l*]P per day for 2 days and sacrificed at 24 h after the second carcinogen dose. Finally, a time-course study was conducted and mice were treated with 24 nmol DB[*a*,*l*]P topically into the oral cavity 3 times per week for 5 weeks (the same dose was used before for 38 weeks, which induced oral cancer in mice at 42 weeks after the first dose). Six animals per group were sacrificed at 48 h and 1, 2, and 4 weeks after the last dose. At termination, mice were sacrificed by CO_2 asphyxiation and soft tissues of the oral cavity including hard palate, buccal mucosa, and floor of mouth, were collected.

DNA was isolated using the Qiagen genomic DNA isolation procedure. Prior to enzymatic digestion, 200 pg of each [$^{15}N_5$]-labeled DB[*a*,*l*]PDE-dA or -dG adducts were added to 200 μg DNA. DNA hydrolysis, solid phase extraction were carried out under similar conditions as those previously published.[15]

LC-MS/MS Analysis. The method used for the detection of DB[*a*,*l*]PDE-DNA adducts by LC-MS/MS is identical to our previously published procedure.[15] In brief, the analysis was carried out on an API 3200 LC/MS/MS triple quadrupole mass spectrometer interfaced with an Agilent 1200 series HPLC using an Agilent Extend-C18 5 μm 4.6 × 150 mm column. The electrospray ionization (ESI) was performed in the positive mode. The MS parameters were set as follows: electrospray

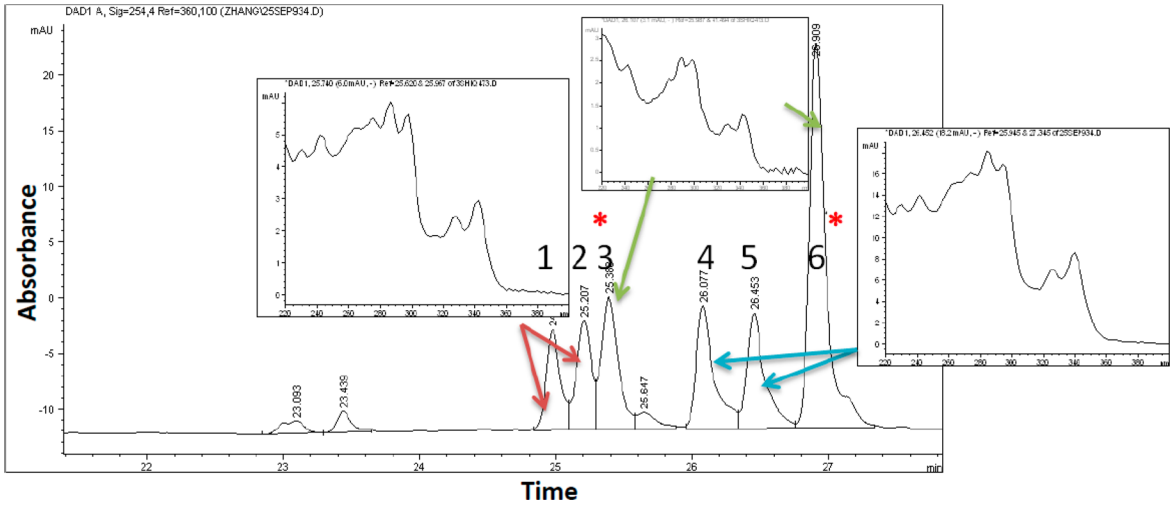

Figure 1. HPLC separation of synthetic DB[*a,l*]PDE-dG adducts. Peaks 1 and 2 have the same UV spectra, Peaks 4 and 5 have the same UV spectra. The absorption of peaks 1 and 2 are shifted 3 nm to longer wavelengths, compared with the absorption of peaks 4 and 5. *: MS analysis showed that peaks 3 and 6 are N^7-Gua adducts.

source temperature and voltage were 400 °C and 5.5 kV, respectively; the declustering potential (DP), collision energy (CE), entrance potential (EP), and cell exit potential (CXP) were optimized as 56, 33, 7.5, and 8eV, respectively; the collision activated dissociation (CAD) gas was set at 5 psi, whereas the curtain gas was set at 20 psi. The elution solvent program was 200 ul/min gradient using solvent A (methanol containing 0.1% formic acid) and solvent B (water containing 0.1% formic acid). The gradient was 10% A to 70% A in 5 min, followed by 70% A in 10 min, continued to 90% A in 30 min, and 90% A was held for another 5 min. Adducts were monitored in multiple reaction monitoring (MRM) mode. The MS/MS transitions of m/z 604→ m/z 335, and m/z 609→ m/z 335 were monitored for dA adducts and their internal standards, respectively. The MS/MS transitions monitored at m/z 620 $[M + H]^+$→ m/z 504 $[(M+H)^+$- 2′-deoxyribose] for DB[*a,l*]PDE-N^2-dG adducts and m/z 625→ m/z 509 for the its ^{15}N-labeled internal standard.

Calibration Curves for DNA Adducts. Calibration curves were constructed by mixing authentic unlabeled adduct (20, 50, 200, and 500 pg), 200 pg of N^{15} internal standard adduct and 100 μg of DNA obtained from oral tissues of untreated mice. As described above, the mixture was subjected to the same DNA digestion and adduct purification procedure for HPLC-MS/MS analysis as described above.

RESULTS

Detection and Identification of dG Adducts Derived from DB[*a,l*]PDE *in Vitro*. HPLC analysis, UV, MS, NMR, and CD spectra were used to detect and identify dG adducts derived from DB[*a,l*]PDE *in vivo*. The four synthetic stereoisomeric adducts formed from the incubation of (±)-*anti*-DB[*a,l*]PDE with dG were prepared as described;[16] a representative HPLC−UV chromatogram of the reaction mixture is shown in Figure 1. On the basis of the MS analysis, peaks 1, 2, 4, and 5 were identified as N^2-dG adducts, formed by reaction of DB[*a,l*]PDE with the $-NH^2$ group at the 2-position of dG. According to a previous report by Li et al. and based on our MS analysis,[16] peaks 3 and 6 were identified as N^7-Gua adducts, formed by reaction of DB[*a,l*]PDE with the N^7 of dG leading to depurinated adducts. Fractions containing DB[*a,l*]PDE-N^2-dG adducts were collected and the structure and stereochemistry of the adducted stereoisomers were identified and characterized by a combination of MS, NMR, and CD spectra. Full MS-ESI scans of DB[*a,l*]PDE-N^2-dG adducts were conducted at the positive mode, indicating the presence of a protonated molecular ion $[M + H]^+$ at m/z 620 (Figure S1 in the Supporting Information). The fragmentation patterns of the molecular ions are similar among these adducts with the presence of m/z 504, 353, 335, 317, 307, with fragment 335 being the strongest signal. The MS/MS fragments of stable isotope labeled internal standards [$^{15}N_5$]-DB[*a,l*]PDE-dG [$(M + H)^+$ at m/z 625] were similar to those of the unlabeled adducts.

The CD spectra were acquired to determine the stereochemistry of each of the N^2-dG adducts (Figure S2 in the Supporting Information). Peak 1 and peak 2 are enantiomers to each other; peak 4 and peak 5 are enantiomers to each other. Each pair of enantiomeric adducts exhibited symmetrical CD spectra, but with opposite signs. Our CD spectra of the four N^2-dG adducts are consistent to those reported by Dreij et al.[19]

The ^1H NMR spectra of peak 1 and peak 5 were obtained to determine the stereochemistry (*cis* vs *trans*) of each diastereomer (Table S1 in the Supporting Information). The chemical shift of the bay or fjord region benzylic methane proton, at the site of attachment to the purine is a diagnostic feature for the assignment of stereochemistry.[20,21] It has been consistently observed that similar marked downfield shifts of the fjord or bay region benzylic proton signal can be used to differentiate the *cis* from the *trans* diastereomers both for dA and dG adducts derived from a number of different PAHs.[21] In the case of DB[*a,l*]PDE, a downfield shift of C_{14}−H for peak 1 is compared to peak 5, that indicate that peaks 1 and 2 are *cis*-N^2-dG adducts; peaks 4 and 5 are *trans*-N^2-dG adducts.

According to the empirical rules established previously for other hydrocarbons, the sign of the signal at ∼270 nm of CD spectra was used to assign the empirical configuration.[20,21] The *cis*- and *trans*- adducted diastereomers with *S* absolute configurations for the benzylic carbon, where the purine is attached, have a positive sign for this band, whereas the *cis* and *trans* diastereomers with *R* absolute configuration have a negative sign. In terms of the elution order (Figure 1), the four

dx.doi.org/10.1021/tx5001078 | *Chem. Res. Toxicol.* 2014, 27, 1199−1206

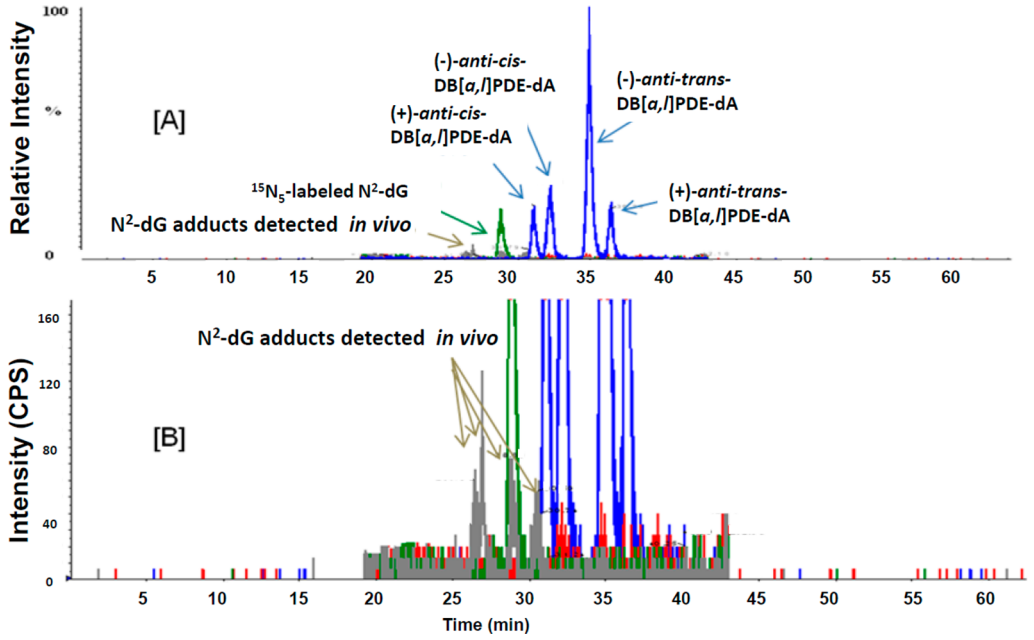

Figure 2. Detection of DB[*a,l*]PDE-N^6-dA and DB[*a,l*]PDE-N^2-dG adducts from oral tissues of mice treated with (±)-*anti*-DB[*a,l*]PDE by HPLC-MS/MS (A). Panel B is the enlarged portion of panel A. Peaks in blue: N^6-dA adducts detected in vivo; peaks in gray: N^2-dG adducts detected in vivo; peak in green: N^{15} internal standards for N^2-dG adduct.

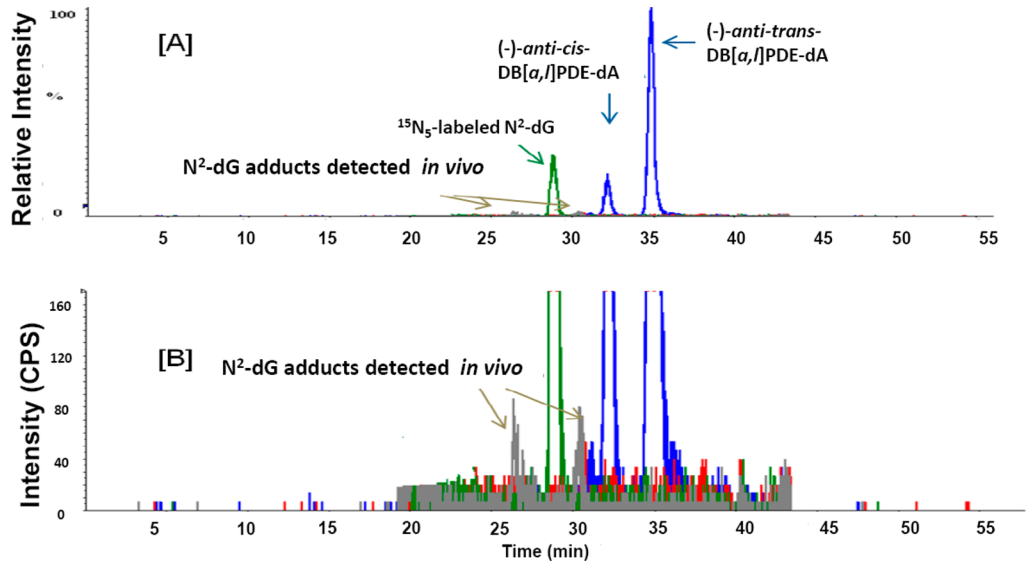

Figure 3. Detection of DB[*a,l*]PDE-N^6-dA and DB[*a,l*]PDE-N^2-dG adducts from oral tissues of mice treated with DB[*a,l*]P by HPLC-MS/MS (A). Panel B is the enlarged portion of panel A. Peaks in blue: N^6-dA adducts detected *in vivo*; peaks in gray: N^2-dG adducts detected *in vivo*; peak in green: N^{15} internal standards for N^2-dG adduct.

synthetic adducts are assigned as (−)-*anti-cis*-, (+)-*anti-cis*-, (+)-*anti-trans*- and (−)-*anti-trans*-DB[*a,l*]PDE-N^2-dG adducts, respectively. In addition, the UV spectra of peak 1 and peak 2 are identical, with the maxima absorption at 325 and 340 nm; whereas peak 4 and peak 5 have the same UV spectra with the maxima absorption at 323 and 338 nm (Figure 1). This is consistent with the report by Dreij et al. indicating that the UV absorption of *cis*-adducts is shifted to longer wavelengths.[22] The $^{15}N_5$-labeled (−)-*anti-cis*- and (−)-*anti-trans*-DB[*a,l*]PDE-N^2-dG were used as internal standards to quantify DB[*a,l*]PDE-N^2-dG adducts in oral tissue of mice treated with DB[*a,l*]P by HPLC-MS/MS (Figure S3 in the Supporting Information).

Identification and Quantification of DB[*a,l*]PDE-dG and DB[*a,l*]PDE-dA Adducts in Oral and Tongue Tissues of Mice Treated with DB[*a,l*]P and DB[*a,l*]PDE. The LC-MS/MS method was used to identify DNA adducts following topical application of (±)-*anti*-DB[*a,l*]PDE into the oral cavity of mice. This method revealed the formation of four dA and four dG adducts in the oral tissues (Figures 2A and 2B). In contrast, we detected two dA and two dG adducts in oral tissues of mice treated with its parent compound, DB[*a,l*]P (Figures 3A and 3B). On the basis of cochromatography of the internal standards with analytes, we identified (−)-*anti-cis* and (−)-*anti-trans*-DB[*a,l*]PDE-N^2-dG adducts and consistent with our previous report,[15] we identified (−)-*anti-cis* and (−)-*anti-*

dx.doi.org/10.1021/tx5001078 | *Chem. Res. Toxicol.* 2014, 27, 1199−1206

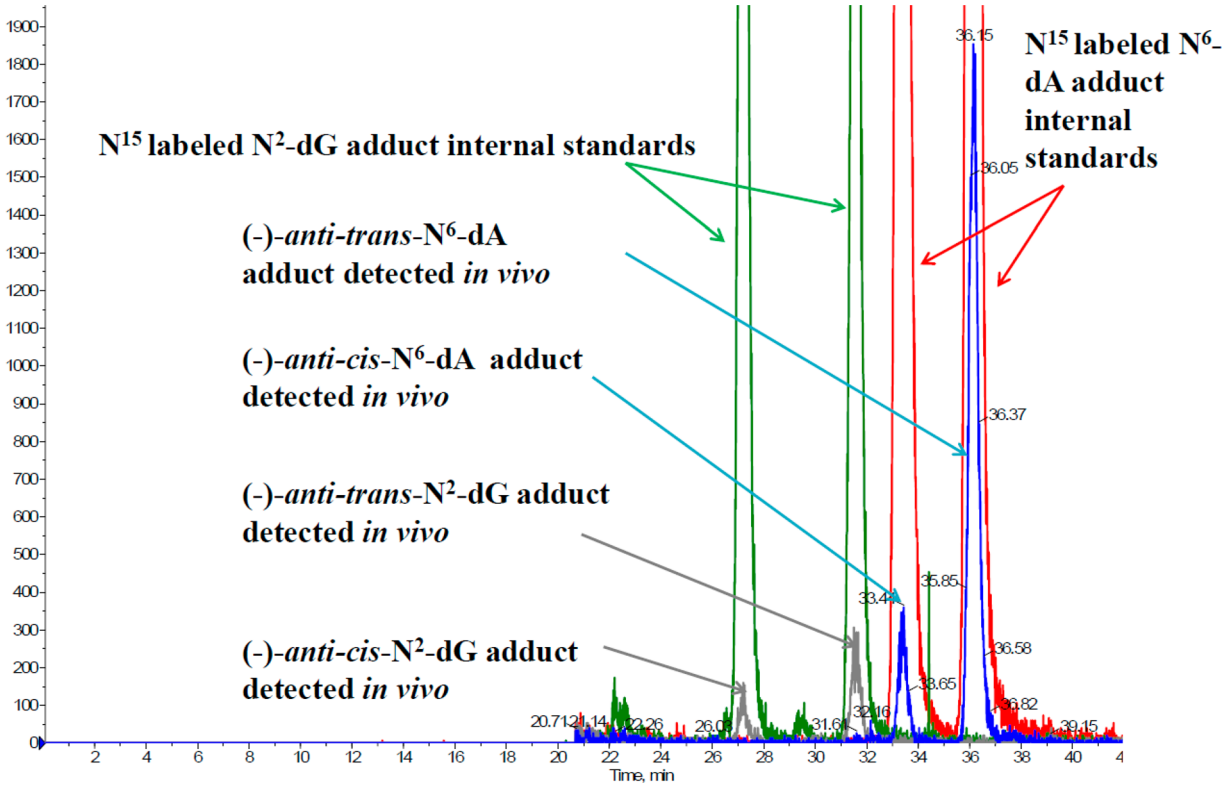

Figure 4. Detection of DB[*a*,*l*]PDE-dA and -dG adducts from oral cavity of mice treated with DB[*a*,*l*]P. Co-elution of internal standards with adducts detected.

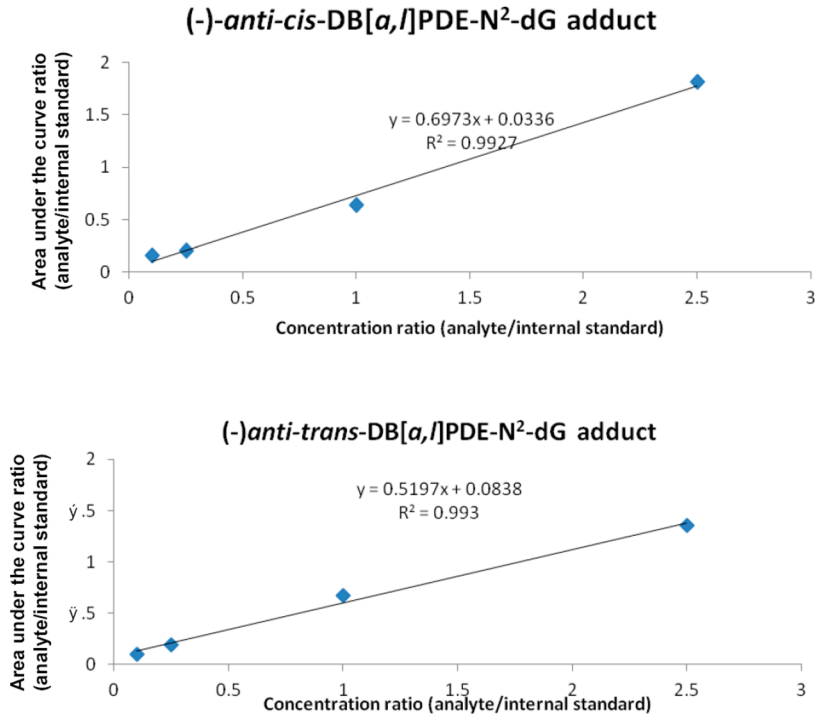

Figure 5. Standard curves for DB[*a*,*l*]PDE-N^2-dG adducts.

trans-DB[*a*,*l*]PDE-N^6-dA adducts (Figure 4). Our results further support that DB[*a*,*l*]P is mainly metabolized to (−)-*anti*-DB[*a*,*l*]PDE in oral cavity of mice. Therefore, Calibration curves were then constructed for the two (−)-*anti-cis*-DB[*a*,*l*]PDE-dG and (−)-*anti-trans*-DB[*a*,*l*]PDE-dG adducts in the presence of 100 μg digested DNA as the matrix. Calibration curves for both adducts are linear (r^2 = 0.9927 and r^2 = 0.993, respectively illustrated in Figure 5). Calibration curves for dA adducts were constructed as previously reported.[15] Because of the expected low levels of dG adducts as depicted in Figures 2−4, we pooled all the oral tissues of mice (n = 3) within the same group, and thus one

dx.doi.org/10.1021/tx5001078 | *Chem. Res. Toxicol.* 2014, 27, 1199−1206

value is reported for each time point. Subsequently, we have determined the levels of DB[*a,l*]PDE-dG and -dA adducts in a time-dependent manner in the oral tissues of mice at 2 days and 1, 2, and 4 weeks after last dose of DB[*a,l*]P treatment (Figure 6A). A representative HPLC-MS/MS chromatogram is shown to demonstrate the quantification of DNA adducts detected *in vivo* (Figure 7). The levels of (−)-*anti-trans*-DB[*a,l*]PDE-dA adduct exceeded that of (−)-*anti-cis*-DB[*a,l*]PDE-dA, (−)-*anti-trans*-DB[*a,l*]PDE-dG as well as (−)-*anti-cis*-DB[*a,l*]PDE-dG adducts at each time point.

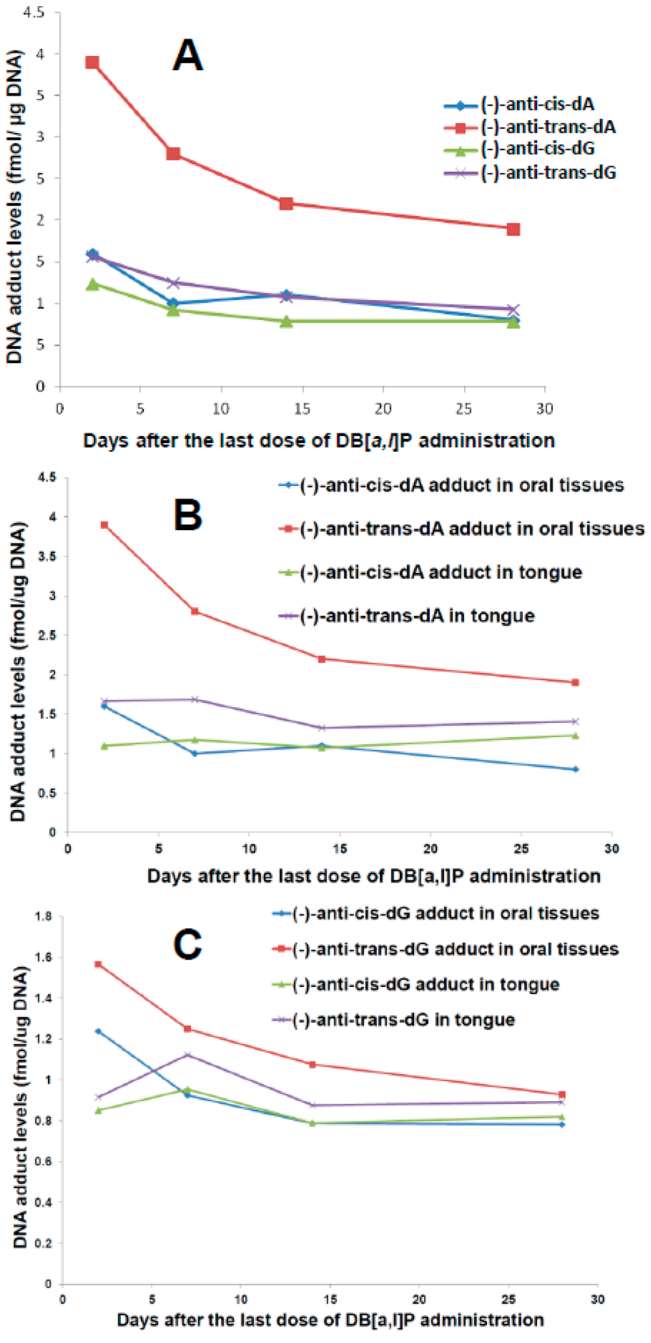

Figure 6. Comparison of DB[*a,l*]PDE-dG and -dA adduct levels in oral tissues of mice treated with DB[*a,l*]P (A). Comparison of DB[*a,l*]PDE-N^6-dA adduct levels in oral tissues and tongue (B) and comparison of DB[*a,l*]PDE-N^2-dG adduct levels in oral tissues and tongue (C) of mice. All tissues were collected at 2 days and 1, 2, and 4 weeks after the last dose of DB[*a,l*]P treatment (24 nmol, 3 times per week, for 5 weeks). Tissues from three mice were pooled at each time point.

In our previous report, we demonstrated that DB[*a,l*]P induced SCC in the oral tissues but not in the tongue while its diol epoxide induced SCC in both oral and tongue tissues.[11] Therefore, in the present study we have compared the levels of dA and dG adducts in oral and tongue tissues of mice treated with DB[*a,l*]P (Figures 6B and C). The levels of (−)-*anti-trans*-DB[*a,l*]PDE-dA adduct in oral tissues exceeded those in tongue at all time points. Levels of (−)-*anti-trans*-DB[*a,l*]PDE-N^2-dA were ≥2 folds higher than (−)-*anti-cis*-DB[*a,l*]PDE-N^2-dA adduct and those of dG adducts in the oral tissues and tongue at all time points after the cessation of DB[*a,l*]P treatment. However, levels of dG adducts were comparable at all time points in both tissues.

DISCUSSION

Using LC-MS/MS analysis, our results clearly demonstrate that following the topical application of multiple doses of DB[*a,l*]P, we were able to simultaneously detect and quantify dG and dA adducts derived from (−)-*anti*-DB[*a,l*]PDE in the oral tissue of mice; levels of (−)-*anti-trans*-N^6-dA adducts exceeded all other DNA lesions detected in this study. In a previous study, Dreij et al. exposed A549 human epithelial lung carcinoma cells to 0.1 µM (±)-*anti*-DB[*a,l*]PDE, levels of DNA adducts were analyzed by HPLC-Fluorescence detector at different time points post-treatment up to 6 h.[22] These authors observed that independent of the concentration and incubation time of DB[*a,l*]PDE, levels of dA adducts were higher than levels of dG, and the ratio of dA and dG adducts remains constant (~2.8) over the time points selected in this study; however, they also observed that within each type of adducts, differences in the rate of adduct removal exist. In another report using ^{32}P-postlabeling analysis, when A/J mouse was treated with DB[*a,l*]P, Prahalad et al. have shown that the predominant adducts in the mouse lung were coeluted with adducts derived from the reaction of *anti*-DB[*a,l*]PDE and dA.[23] These results appear to be consistent with our observations that (−)-*anti-trans*-DB[*a,l*]PDE-dA is the major DNA adduct detected in the oral tissues of mice treated with DB[*a,l*]P, and therefore, the level of this adduct may be causally related to the oral carcinogenicity of DB[*a,l*]P.[11] Furthermore, our results demonstrate the levels of these adducts were higher in the oral tissues than in the tongue of mice treated with DB[*a,l*]P, which may, in part, account for the carcinogenicity of DB[*a,l*]P in the oral tissues but not in the tongue.

Interestingly, Spencer et al. demonstrated that guanine adducts detected by ^{32}P-postlabeling were the major adducts following the incubation of cell lines with racemic (±)-*anti*-DB[*a,l*]PDE, and these adducts were particularly refractory to the removal by nucleotide excision repair (NER) system in several human NER proficient (NER^+) cell lines.[24] However, the *in vitro* reaction of DNA with the parent compound DB[*a,l*]P in the presence of rat liver microsomes, resulted in dA: dG adducts in nearly 1:1 ratio.[25,26] Furthermore, other studies have shown that (−)-*anti*-DB[*a,l*]PDE reacts predominantly with adenine in human epithelial cells, resulting primarily in mutations at A:T base pairs.[22] On the basis of these studies, it is likely that (+)-*anti*-DB[*a,l*]PDE is responsible for the large numbers of dG adducts formed in studies by Spencer et al. when those human cell lines were treated with 1 nM (±)-*anti*-DB[*a,l*]PDE.[24] The variations in the levels of dA and dG adducts among different studies may be due to different doses,

dx.doi.org/10.1021/tx5001078 | *Chem. Res. Toxicol.* 2014, 27, 1199−1206

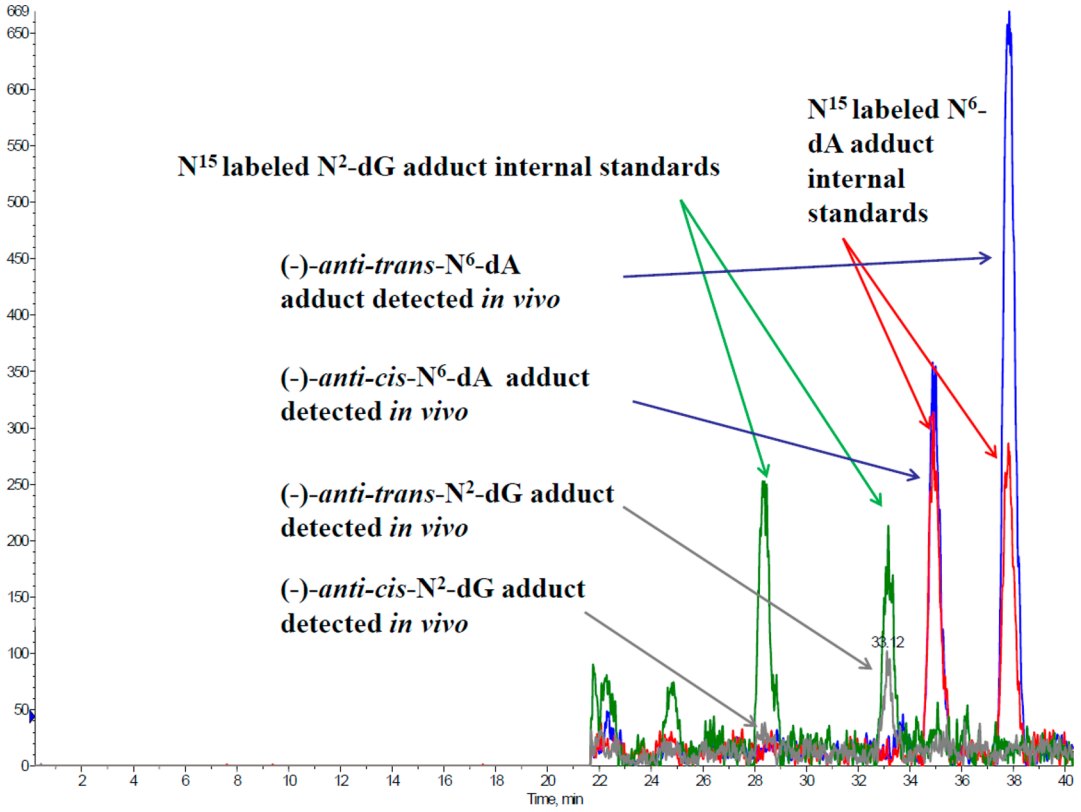

Figure 7. Representative LC-MS/MS chromatography for the quantification of DB[*a*,*l*]PDE-dG and -dA adducts in oral tissues of mice treated with DB[*a*,*l*]P.

differences in metabolic capacities of various cell types *in vitro* and *in vivo*, route of adminstration, or treatment duration as well as time points of those measurements.

DB[*a*,*l*]P was mutagenic in the oral cavity of the big blue mice; it induced high fractions of G:C → T:A and G:C → A:T substitutions, besides a significant higher fraction (31%) at AT base pairs compared with the mutation profile induced by B[*a*]P.[11] In our opinion, although fjord region diol epoxides (e.g., DB[*a*,*l*]PDE) prefer to form higher levels of dA adducts than dG adducts, certain dG adducts may be resistant to NER; thus, the simultaneous detection of dA and dG adducts derived from DB[*a*,*l*]P is necessary to explore the mechanisms that can account for the oral carcinogenesis induced by this carcinogen. In our previous report, we showed that DB[*a*,*l*]P-induced SCC in oral tissues but not in the tongue after direct application of DB[*a*,*l*]P into the oral cavity;[11] however, DB[*a*,*l*]PDE is a potent carcinogen in both oral tissues and tongue.[13] Toward this end, we initially focused on DB[*a*,*l*]P-induced genotoxic effects in this target organ. Among all the DB[*a*,*l*]P-induced dA and dG adducts examined, the level of (−)-*anti-trans*-DB[*a*,*l*]PDE-dA was clearly higher in oral tissues than in tongue at all time points. As we stated earlier that the level of (−)-*anti-trans*-DB[*a*,*l*]PDE-dA is important in DB[*a*,*l*]P-induced oral carcinogenesis, our results are consistent with our previous finding that DB[*a*,*l*]P induced SCC in the oral tissues but not in the tongue.

■ ASSOCIATED CONTENT

Supporting Information

MS/MS fragment of anti-DB[*a*,*l*]PDE-dG and [$^{15}N_5$]-anti-DB[*a*,*l*]PDE-dG. CD spectral analysis to assign stereochemistry of adducts. Table of NMR data. LC-MS/MS chromatogram of the $^{15}N_5$-labeled (−)-*anti-cis*- and (−)-*anti-trans*-DB[*a*,*l*]PDE-N^2-dG. This material is available free of charge via the Internet at http://pubs.acs.org.

■ AUTHOR INFORMATION

Corresponding Author

*K. El-Bayoumy. E-mail: kee2@psu.edu. Tel.: 717-531-1005. Fax: 717-531-0002. Address: Department of Biochemistry and Molecular Biology, Pennsylvania State College of Medicine, Hershey, PA 17033, United States.

Author Contributions

§The authors have equally contributed to this manuscript.

Funding

Grant Support: by NCI grant R01-CA173465 and NIEHS R21ES020411.

Notes

The authors declare no competing financial interest.

■ ABBREVIATIONS

DB[*a*,*l*]P, dibenzo[*a*,*l*]pyrene; DB[*a*,*l*]PDE, (±)-*anti*-11,12-dihydroxy-13,14-epoxy-11,12,13,14-tetrahydrodibenzo[*a*,*l*]-pyrene; PAH, polycyclic aromatic hydrocarbon; dA, deoxyadenosine; dG, deoxyguanosine; NER, nucleotide excision repair

■ REFERENCES

(1) American Cancer Society (2013) *Cancer Facts & Figures*, pp 17−18, American Cancer Society, Atlanta, GA.

(2) Mallery, S. R., Tong, M., Michaels, G. C., Kiyani, A. R., and Hecht, S. S. (2014) Clinical and Biochemical Studies Support

Smokeless Tobacco's Carcinogenic Potential in the Human Oral Cavity. *Cancer Prev. Res. 7*, 23−32.
(3) United States Surgeon General (2010) *How Tobacco Smoke Causes Disease: The Biology and Behavioral Basis for Smoking-Attributable Disease: A Report of the Surgeon General*, Surgeon General, Rockville, MD.
(4) Harvey, R. G. (1991) *Polycyclic aromatic hydrocarbons: chemistry and carcinogenicity*, Cambridge University Press, Cambridge.
(5) Krzeminski, J., Lin, J. M., Amin, S., and Hecht, S. S. (1994) Synthesis of Fjord region diol epoxides as potential ultimate carcinogens of dibenzo[a,l]pyrene. *Chem. Res. Toxicol. 7*, 125−129.
(6) Luch, A. (2009) On the impact of the molecule structure in chemical carcinogenesis. *EXS 99*, 151−179.
(7) Luch, A., Coffing, S. L., Tang, Y. M., Schneider, A., Soballa, V., Greim, H., Jefcoate, C. R., Seidel, A., Greenlee, W. F., Baird, W. M., and Doehmer, J. (1998) Stable expression of human cytochrome P450 1B1 in V79 Chinese hamster cells and metabolically catalyzed DNA adduct formation of dibenzo[a,l]pyrene. *Chem. Res. Toxicol. 11*, 686−695.
(8) Snook, M. E., Severson, R. F., Arrendale, R. F., Higman, H. C., and Chortyk, O. T. (1977) Identification of High Molecular-Weight Polynuclear Aromatic-Hydrocarbons in a Biologically-Active Fraction of Cigarette-Smoke Condensate. *Beitr. Tabakforsch. 9*, 79−101.
(9) Buters, J. T., Mahadevan, B., Quintanilla-Martinez, L., Gonzalez, F. J., Greim, H., Baird, W. M., and Luch, A. (2002) Cytochrome P450 1B1 determines susceptibility to dibenzo[a,l]pyrene-induced tumor formation. *Chem. Res. Toxicol. 15*, 1127−1135.
(10) Chen, K. M., Zhang, S. M., Aliaga, C., Sun, Y. W., Cooper, T., Gowdahalli, K., Zhu, J., Amin, S., and El-Bayoumy, K. (2012) Induction of ovarian Cancer and DNA adducts by dibenzo[a,l]pyrene in the mouse. *Chem. Res. Toxicol. 25*, 374−380.
(11) Guttenplan, J. B., Kosinska, W., Zhao, Z. L., Chen, K. M., Aliaga, C., DelTondo, J., Cooper, T., Sun, Y. W., Zhang, S. M., Jiang, K., Bruggeman, R., Sharma, A. K., Amin, S., Ahn, K., and El-Bayoumy, K. (2012) Mutagenesis and carcinogenesis induced by dibenzo[a,l]pyrene in the mouse oral cavity: a potential new model for oral cancer. *Int. J. Cancer 130*, 2783−2790.
(12) IARC Working Group on the Evaluation of Carcinogenic Risks to Humans (2010) Some non-heterocyclic polycyclic aromatic hydrocarbons and some related exposures. *IARC Monogr. Eval. Carcinog. Risks Hum. 92*, 1−853.
(13) Chen, K. M., Guttenplan, J. B., Zhang, S. M., Aliaga, C., Cooper, T. K., Sun, Y. W., DelTondo, J., Kosinska, W., Sharma, A. K., Jiang, K., Bruggeman, R., Ahn, K., Amin, S., and El-Bayoumy, K. (2013) Mechanisms of oral carcinogenesis induced by dibenzo[a,l]pyrene: an environmental pollutant and a tobacco smoke constituent. *Int. J. Cancer 133*, 1300−1309.
(14) Zhao, L., Balbo, S., Wang, M., Upadhyaya, P., Khariwala, S. S., Villalta, P. W., and Hecht, S. S. (2013) Quantitation of pyridyloxobutyl-DNA adducts in tissues of rats treated chronically with (R)- or (S)-N′-nitrosonornicotine (NNN) in a carcinogenicity study. *Chem. Res. Toxicol. 26*, 1526−1535.
(15) Zhang, S. M., Chen, K. M., Aliaga, C., Sun, Y. W., Lin, J. M., Sharma, A. K., Amin, S., and El-Bayoumy, K. (2011) Identification and quantification of DNA adducts in the oral tissues of mice treated with the environmental carcinogen dibenzo[a,l]pyrene by HPLC-MS/MS. *Chem. Res. Toxicol. 24*, 1297−1303.
(16) Li, K. M., George, M., Gross, M. L., Lin, C. H., Jankowiak, R., Small, G. J., Seidel, A., Kroth, H., Rogan, E. G., and Cavalieri, E. L. (1999) Structure elucidation of the adducts formed by fjord resell dibenzo[a,l]pyrene-11,12-dihydrodiol 13,14-epoxides with deoxyguanosine. *Chem. Res. Toxicol. 12*, 778−788.
(17) Sharma, A. K., Kumar, S., and Amin, S. (2004) A Highly Abbreviated Synthesis of Dibenzo[def,p]chrysene and Its 12-Methoxy Derivative, a Key Precursor for the Synthesis of the Proximate and Ultimate Carcinogens of Dibenzo[def,p]chrysene. *J. Org. Chem. 69*, 3979−3982.
(18) Sundberg, K., Dreij, K., Seidel, A., and Jernstrom, B. (2002) Glutathione conjugation and DNA adduct formation of dibenzo[a,l]-pyrene and benzo[a]pyrene diol epoxides in V79 cells stably expressing different human glutathione transferases. *Chem. Res. Toxicol. 15*, 170−179.
(19) Dreij, K., Bajak, E., Sundberg, K., Cotgreave, I., Jernstrom, B., Seidel, A., and Gusnanto, A. (2004) DNA adducts of benzo[a]pyrene- and dibenzo[a,l]pyrene-diol epoxides in human lung epithelial cells: Kinetics of adduct removal, effects on cell cycle checkpoints, and gene expression. *Polycyclic Aromat. Compd. 24*, 549−566.
(20) Yagi, H., Frank, H., Seidel, A., and Jerina, D. M. (2008) Revised assignment of absolute configuration of the cis- and trans-N6-deoxyadenosine adducts at C14 of (±)-11beta,12alpha-dihydroxy-13alpha,14alpha-epoxy-11,12,13,14-tetrahydrodibenz o[a,l]pyrene by stereoselective synthesis. *Chem. Res. Toxicol. 21*, 2379−2392.
(21) Szeliga, J., and Dipple, A. (1998) DNA adduct formation by polycyclic aromatic hydrocarbon dihydrodiol epoxides. *Chem. Res. Toxicol. 11*, 1−11.
(22) Dreij, K., Seidel, A., and Jernstrom, B. (2005) Differential removal of DNA adducts derived from anti-diol epoxides of dibenzo[a,l]pyrene and benzo[a]pyrene in human cells. *Chem. Res. Toxicol. 18*, 655−664.
(23) Prahalad, A. K., Ross, J. A., Nelson, G. B., Roop, B. C., King, L. C., Nesnow, S., and Mass, M. J. (1997) Dibenzo[a,l]pyrene-induced DNA adduction, tumorigenicity, and Ki-ras oncogene mutations in strain A/J mouse lung. *Carcinogenesis 18*, 1955−1963.
(24) Spencer, W. A., Singh, J., and Orren, D. K. (2009) Formation and differential repair of covalent DNA adducts generated by treatment of human cells with (±)-anti-dibenzo[a,l]pyrene-11,12-diol-13,14-epoxide. *Chem. Res. Toxicol. 22*, 81−89.
(25) Arif, J. M., Smith, W. A., and Gupta, R. C. (1997) Tissue distribution of DNA adducts in rats treated by intramammillary injection with dibenzo[a,l]pyrene, 7,12-dimethylbenz[a]anthracene and benzo[a]pyrene. *Mutat. Res. 378*, 31−39.
(26) Todorovic, R., Devanesan, P., Rogan, E., and Cavalieri, E. (2005) Identification and quantification of stable DNA adducts formed from dibenzo[a,l]pyrene or its metabolites in vitro and in mouse skin and rat mammary gland. *Chem. Res. Toxicol. 18*, 984−990.